$ZnCo_2O_4$ an efficient electrode material for energy storage devices: An overview

Minaj M. Faras[a,b], Annirudhh A. Mohite[a,b], Appasaheb P. Torane[a,b]

[a]*Department of Physics, Yashavantrao Chavan Institute of Science, Satara, Maharastra 415001, India.*

[b]*Rayat Institute of Research and Development, Satara, Maharashtra, 415001, India.*

Corresponding author: Tel.: 919890916766

E-mail address: appasahebtorane@yahoo.in (Appasaheb P. Torane)

Abstract

Supercapacitors provide a greater power efficiency than rechargeable batteries and a greater energy density in comparison with traditional capacitors, Supercapacitors have attracted much more interest in next-generation power storage systems. Because supercapacitors offer a much more power efficiency than batteries and a greater power density than ordinary dielectric capacitors, they have attracted much interest in next-generation power storage systems. The typical cubic spinel (AB_2O_4) structure with Zn-ions at tetrahedral sites and Co-ions at the octahedral position, makes $ZnCo_2O_4$ a better replacement in supercapacitor to deliver the highest capacity. Electrically conductive zinc ions may improve the electrical conductivity and capacitive effectiveness of $ZnCo_2O_4$. Furthermore, due to its modified electrochemistry, $ZnCo_2O_4$ is often used in supercapacitor applications. This review focuses on several research connected to ZCO supercapacitor (SCs), improving the effectiveness of ZCO SCs, and various methods utilized in ZCO SCs fabrication.

Keywords: $ZnCo_2O_4$, supercapacitor, electrolyte, energy density.

1. Introduction

Because of their long cycle stability, high-power density, compact size, rapid charging capabilities, minimal maintenance, safe operation, and eco-friendly features, supercapacitor (SCs) are referred to as the modified options for energy-containing systems in the coming decades. Nonetheless, more dependable, efficient, and nature-friendly, low-cost energy storage devices are required for reusable energy sources. Industrial power grids, military equipment, hybrid electric cars, and other uses have all utilized SCs. SCs' energy density lower, on the other site, precludes usage in a wide range of applications. To resolve this restriction and make SCs equivalent to batteries, the most recent findings are concentrated on improving the energy density of SCs (Guo et. al., 2013; Hou et. al., 2015; Xu et. al., 2014)

Table 1: Details about SCs on the basis of their types and charge storage mechanism.

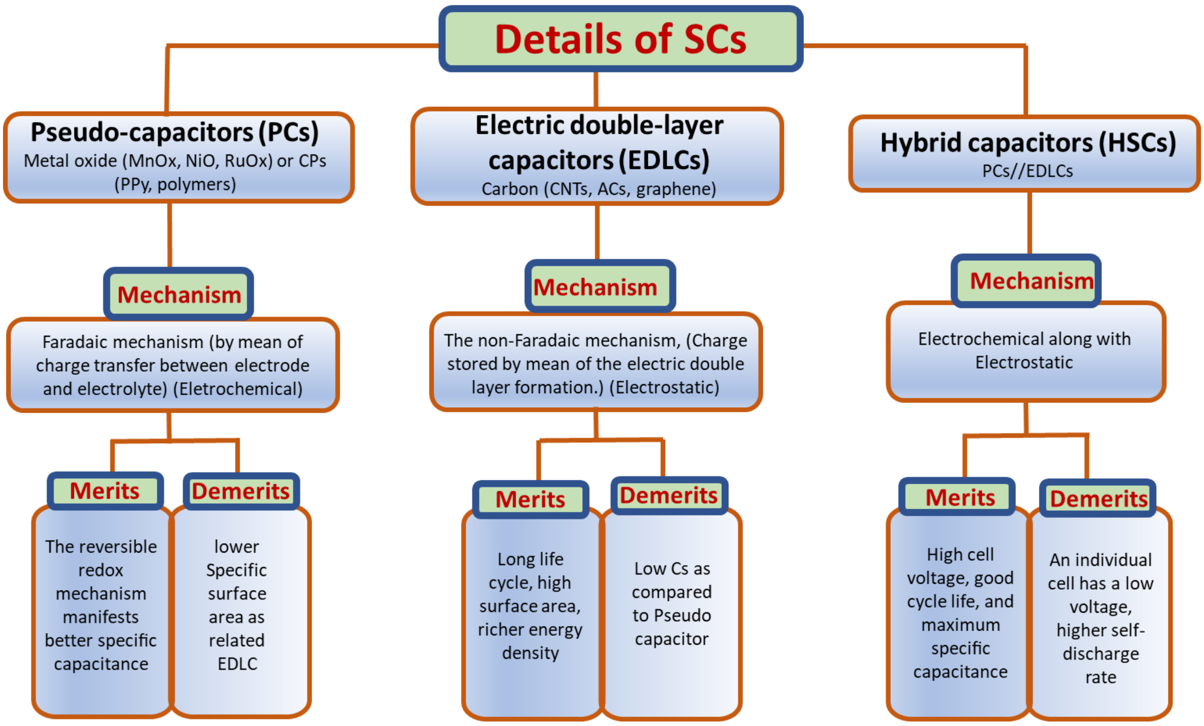

Because of their greater power density, Electrochemical capacitors (ECs) are another name for SCs (Winter and Brodd 2004; Pandolfo and Hollenkamp 2006; Shao et. al., 2012: Zou et. al.,

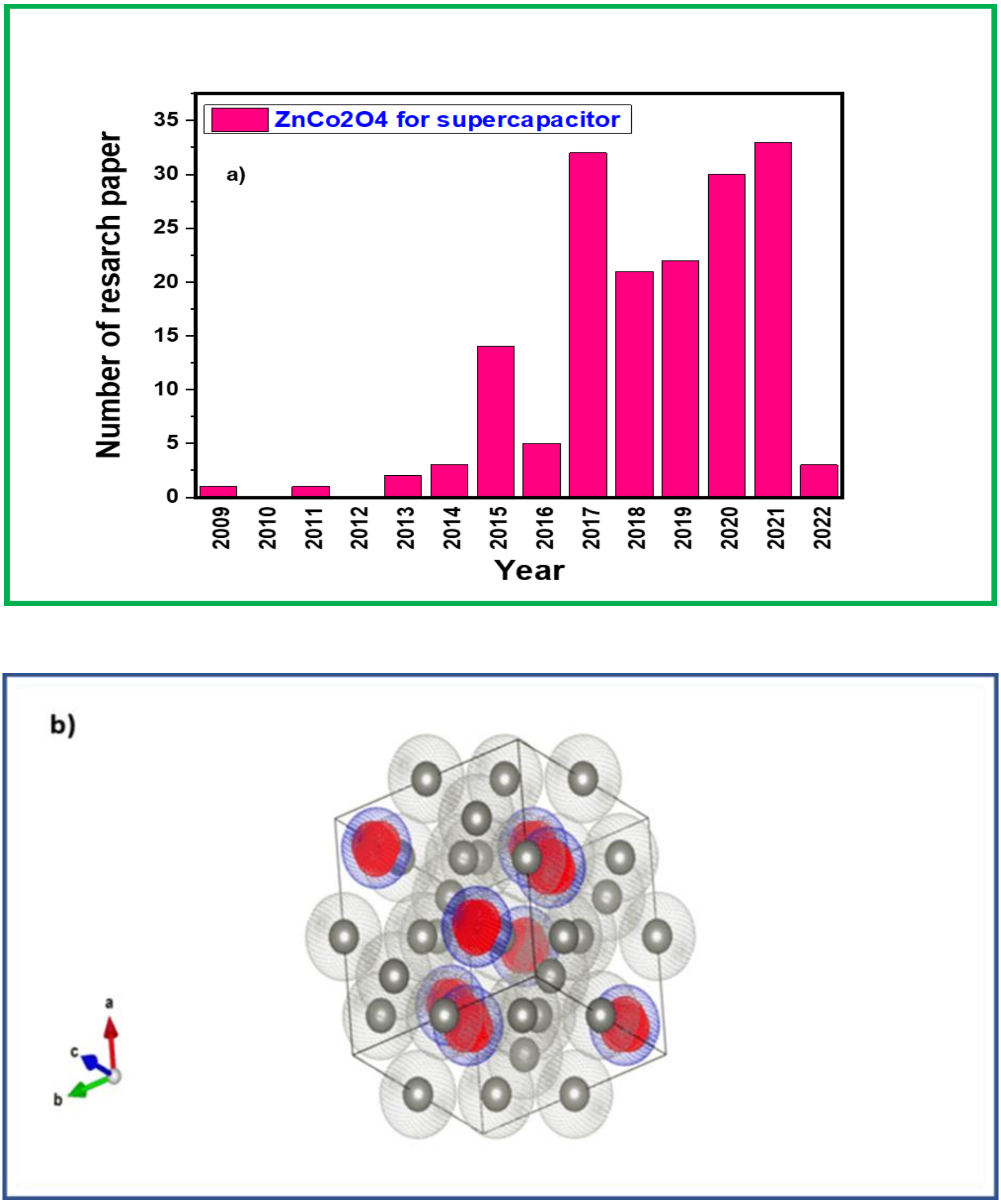

Fig. 1 a) Reported research papers from the year 2009 onwards with search keyword '$ZnCo_2O_4$ for SCs' (www.scopus.com). b) raster image of the crystal structure of Zinc cobaltite.

2013; Xing et. al., 2004). According to the literature, several materials for SC are recently investigated. To have a long cycle life, electrode materials must have a high surface area with excellent structural and mechanical integrity is needed. Carbon-based materials (for example, carbon fibers (CFs) (Leitner et. al., 2006; Leitner et. al., 2006), graphite, & carbon nanotubes CNTs) (Li et. al., 2012; Frackowiak 2000), activated carbons (ACs) (Wei 2012; Kaliaraj and Ramadoss 2020), conducting polymers (CPs) and their derivatives, metal oxides, have all been broadly investigated as an electrode material for SC. Through the existence of Faradaic redox processes, transition metal oxides were shown to have significantly greater specific capacitance (Cs) in a contrast to other types of electrode compounds in terms of their high conceptual capacitance. Iridium oxide (Dubal et. al., 2013), ruthenium oxide (Sugimoto et. al., 2005; Li et. al., 2013), cobalt oxide (Cheng et. al., 2010), manganese oxide (Lu et. al., 2011), zinc oxide (He et. al., 2011), and nickel oxide are some metal oxide-based electrodes which have undergone extensive study. Table 1 lists the different kinds of SCs, as well as their advantages and disadvantages. Fig 1a). Shows from the year 2009 onwards, several articles were published on ZCO material for SC application. Fig 1b) demonstrates the typical crystal image of ZCO, the raster image shows black colored balls located Zn ions, and red-colored 'Co', ions are surrounded by blue 'O' ions balls.

Researchers are using TMOs and conductive polymers to fabricate SCs. As a result, a list of TMOs and polymers were investigated, as potential electrode materials for SCs. They include Co_3O_4, polyaniline, MnO_2, polypyrrole (PPy), and NiO. SCs made of single metal oxide substances, on the other hand, have poor electrical conductivity, decreased energy density, and poor cycle stability, limiting their practical uses. TMOs have gotten a lot of interest in improving SCs because they can improve the redox chemistry of materials like $NiMn_2O_4$, $ZnCo_2O_4$, and $MnCo_2O_4$.

Because of its high theoretical capacity and electrical conductivity, and the fact that from low-cost precursors and earth-abundant materials, ZCO achieved a lot of interest among the different TMOs discussed. A variety of papers on ZCO-based SCs hahaseen published recently, including both conceptual and empirical data. ZCO nanorods Wu et. al., 2019), Micro-flowers and micro-sheets made of ZCO (Pan et. al., 2017), ZCO porous microspheres, and ZCO nanoflakes (Cheng et. al., 2015), Nanosheets, nanotubes, and nanowires of ZCO (Bao et. al., 2014). Sheet-like morphologies with lower thickness and large effective surface area had a much-modified electrical conductivity among the different ZCO morphologies (Chen et. al., 2019). However, to alter the energy density and cyclic stability of SCs, the capacitive material needs to be improved. (Simon and Gogotsi 2010).

ZCO has been examined as a possible functional (anode) material in Li-ion batteries (LIBs) (Chen 2009). It has a cubic spinel (AB_2O_4) nature, with many oxidation states, which shows in a reversible redox reaction that provides extraordinary capacitance (Sharma et. al., 2009). Up to now, a few studies have been done to synthesize a variety of ZCO electrodes as an anode material for LIBs. Such as three-dimensional (3D) nanowire arrays/carbon cloth of ZCO, porous nanoflakes, and one-dimensional (1D) nanoparticles, all of which have high electrochemical activity (Zhang et. al., 2017). However, few types of research on the SCs assessment of ZCO nanostructured electrode materials have been conducted.

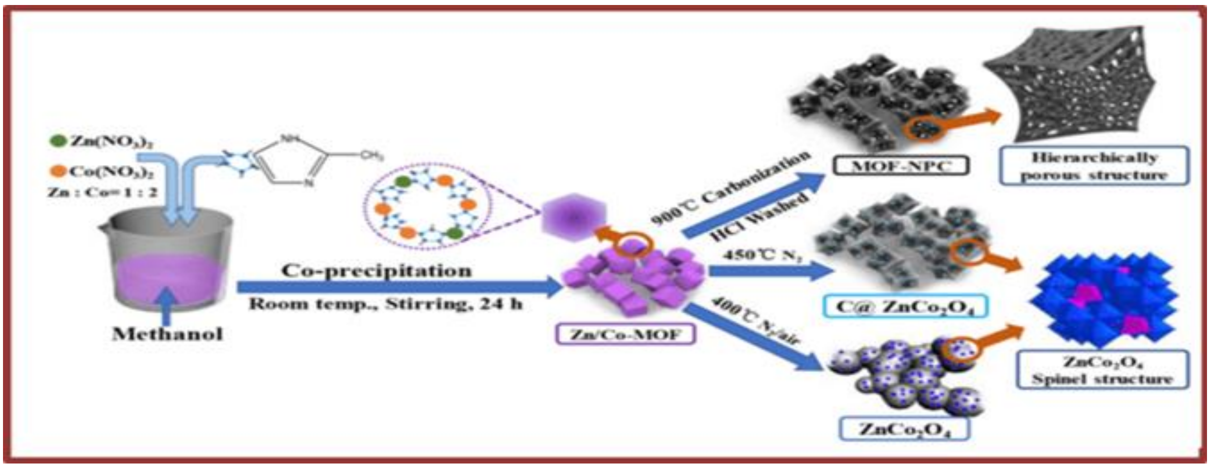

Fig. 2 Diagrammatic illustration for Zinc-based oxides (reproduce with permission).

2. Nanostructured ZCO electrodes with different morphologies:

Morphology is one of the precious parameters for evaluating SCs' performance. Porous morphology helps to increase the performance of SCs by means of a higher specific surface area. According to Zhang X et al., (2017), a two-step hydrothermal technique is used to place fan-shaped $ZnMoO_4$ on flower-like ZCO nanowire arrays. To deposit $ZnMoO_4$ on ZCO, a ZCO nanowire is initially produced and utilized as support. $ZnMoO_4$ completely covers the flower-like ZCO nanowire arrays. When employed as an electrode for an SC with a current density of 1 A/g, this distinctive configuration has higher Cs up to 1506 F/g and excellent cycling capabilities (5000 charge-discharge cycles). Huang et al., (2015) presented a layered structure of ZCO@$NiCo_2O_4$ core-shell nanowires, produced by using a simple co-precipitation technique and easy electrospinning method.

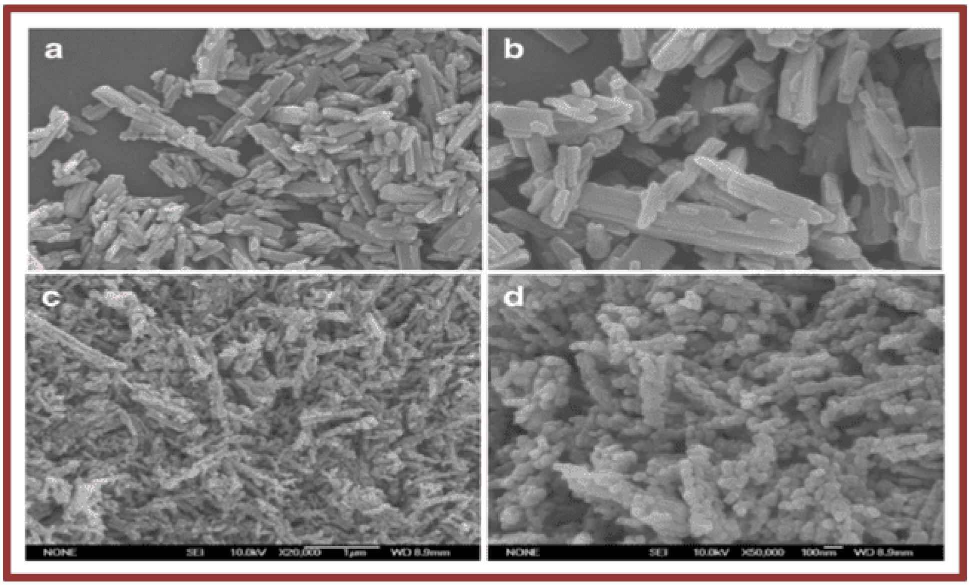

Fig 3. a-d) The SEM images of oxalate precursors and porous ZCO nanorod.

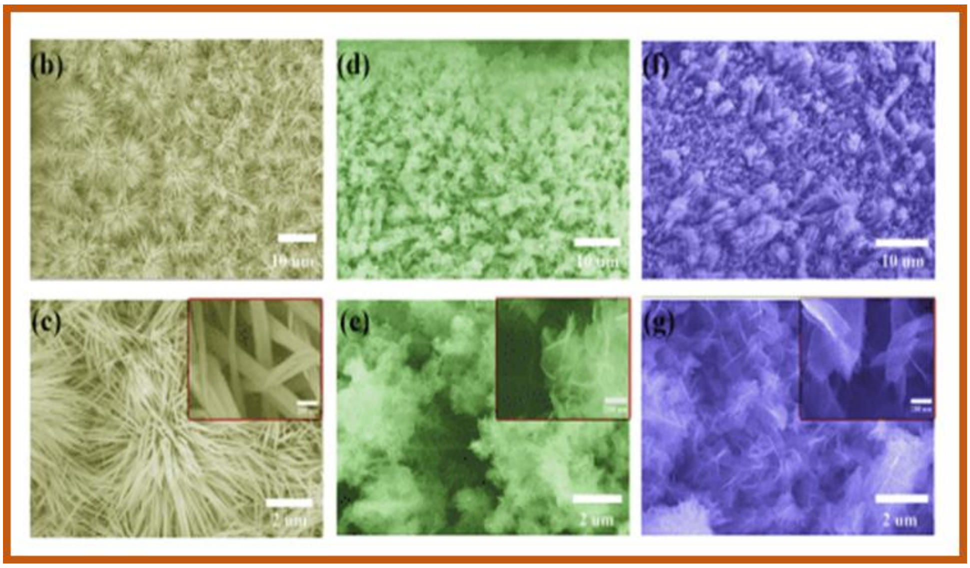

Fig. 4. SEM images of ZCO nanowires

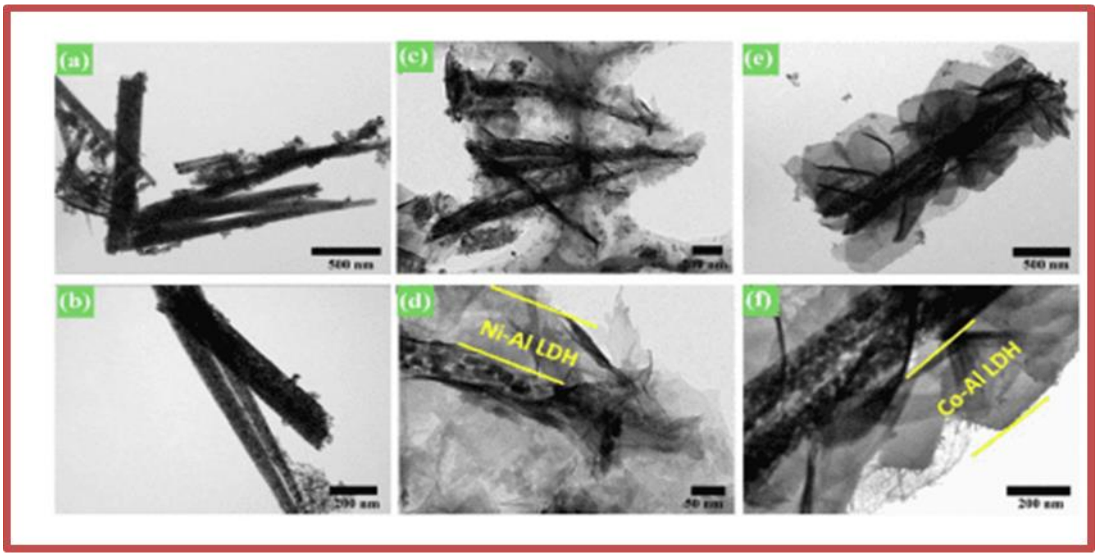

Fig. 5. ZCO via TEM at different magnifications.

3. Different studies on ZCO - based composites:

Transmission electron microscopy (TEM)Tool, GCD technique at various current densities These techniques are used to evaluate the ZCO nanomaterial produced by Karthikeyan K et al., (2009). The crystal structure and surface morphology demonstrate a good impact on the increase of specific capacitance. The SC based on ZCO-cell has an excellent high coulombic efficiency or cycle strength.

Reddy et al., (2020) used a hydrothermal technique using polyvinylpyrrolidone to synthesize 3D-hierarchical peony-like ZCO constructions with 2D-nanoflakes. In the case of ZCO-6h and ZCO-12h electrodes, the obtained discharge time was different, but the remainder of the synthesis parameters remained the same. The outstanding capacitive results point to 3D-ZCO hierarchical peony-like structures that were fabricated using 2D-nanoflakes as a potential substance for elevated efficiency SCs.

Xue Bai et. al., (2019), Using a scalable approach, ZCO nanowires implanted with two types of typical layered double hydroxides are prepared. Fig 4. Shows SEM images of ZCO nanowires with different composites. The core-shell hierarchical structure is seen in both materials. ZCO Co–Al LDH and ZCO@Ni–Al LDH have capacitances of 2041 F/g and 1586 F/g, respectively. The significance of hierarchical structure in improving staging is shown when combined with active surface and synergistic impact. Furthermore, solid-state SCs device using above mentioned manufactured materials as an anode obtained carbon as cathode material, and PVA–KOH as gel electrolyte are demonstrated. ZCO@Co–Al LDH/AC has delivered maximum power and energy efficiencies of 6200 W/kg and 50.1 Wh/kg, respectively. ZCO@Ni–Al LDH/AC has power and energy efficiencies of 3400 W/kg and 27.8 Wh/kg, respectively.

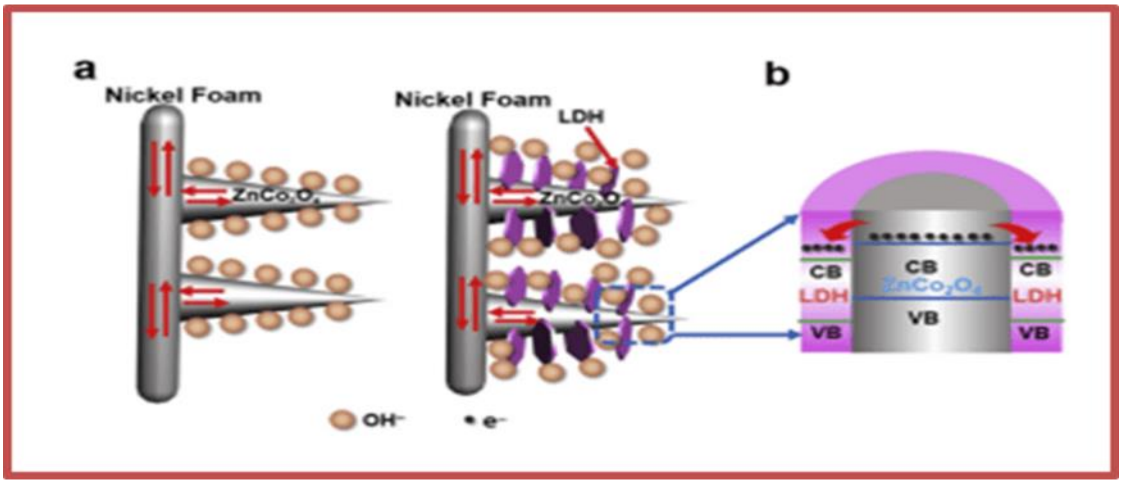

Fig. 6. Structural comparison of ZCO@LDH

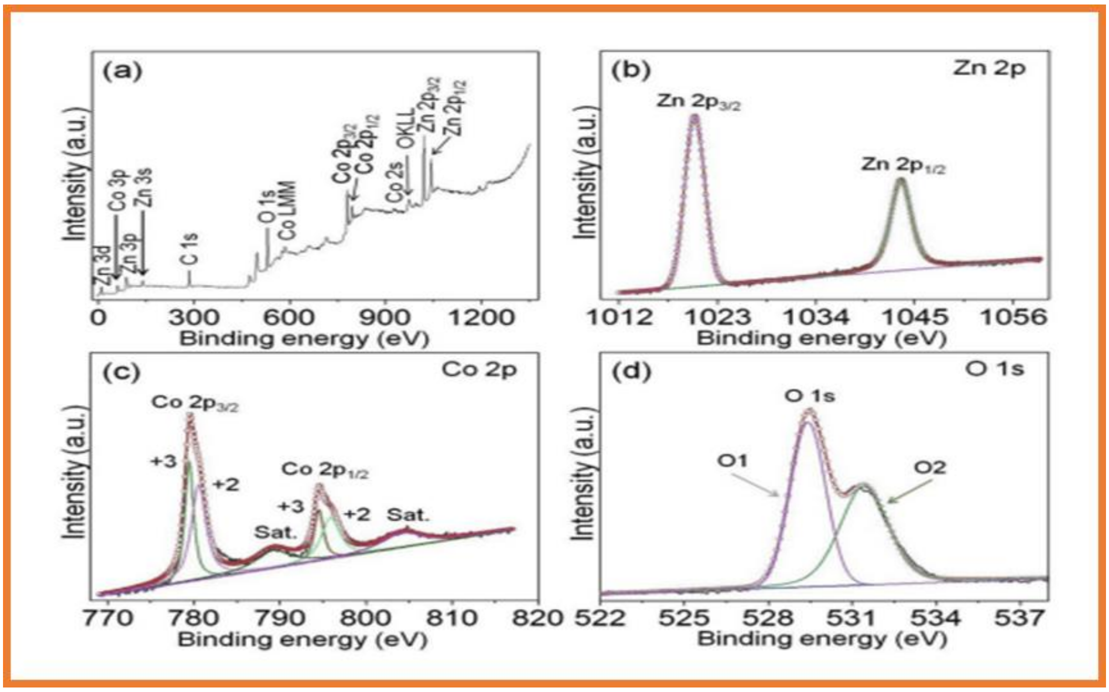

Fig. 7 a- d) XPS study and core-level spectra.

ZCO nanoparticles are produced using a rapid, simple, and cost-effective combustion process, according to Bhagwan J et al., (2020). The impacts of calcination at high temperature on the shape, electrochemical characteristics, & crystallite size of ZCO is investigated. The shape of the produced ZCO is substantially encouraged by the calcination temperature, according to observations made using an SEM. With calcination temperatures of 300, 400, and

600 °C at a current density of 1 A/g, ZCO exhibits Cs of 202, 668, and 843 F/g respectively. Moreover, higher calcination temperatures (800 °C) result in fast particle size increase, lower rate capability of ZCO, and poor Cs that may be related to significant micro-strain and crack development (“432 F/g at 1A/g”).

Huang C et al., (2019) described the manufacturing and rational design of ternary “ZnO/ZCO/NiO” enveloped by nanosheets generated from ZIF-8. NiO composites/ $ZnCo_2O_4$/polyhedral ternary ZnO enclosed by different nanosheets composition of is successfully synthesized by in situ production on ZIF-8 sample & various heat tempering in air. The compound material is denser once the molar mass ratio of nickel to cobalt is 1:1.

Zhao S et al., (2020) used a calcination method to create homogeneous one-dimensional metal oxide hollow tubular nanofibers, researchers used electrospinning nanowires as softer templates or zeolitic imidazolate structure particles as precursors (HTNs). The Co_3O_4 HTNs, ZnO HTNs, and ZCO HTNs were successfully synthesized using the standard synthesis technique. The best ZCO HTNs, when used as the positive electrode in SCs, have an outstanding rate performance of 75.14%. Asymmetric SC made of ZCO HTNs and active carbon also exhibits steady or cycling behavior of ultra-high stability after 20,000 cycles, with 95.38 % of its initial capacity.

Heydari H et al., (2016) used a two-step simple approach to produce ZCO nanoflakes on Ni foam, using the cathodic electrolytic electrodeposition (ELD) method to accompany ied physical characterizations reveal that mesoporous ZCO nanoflakes have good physical stability with Ni foam, and high electroactive surface areas (138.8 m^2/g), allowing for rapid charge transport. The electrochemical characteristics of the ZCO nanoflakes on conducting Ni foam substrate were tested in a 2M KOH aqueous electrolyte solution before they were utilized as consolidated electrodes for SCs.

Using a simple, quick, and cheap hydrothermally aided use without any Ni precursor salt, nanowire networks of $ZnCo_2O_4$/reduced graphene oxide/NiO are in the ternary form primarily on such a part of Ni foam that uses the Thermo annealed method. and as an SC electrode without the need for binding Sahoo S and colleagues (2018). In that sequence, Ni foam has been used as a NiO precursor, adhesive, as well as recent collector. Obtained 3D ternary composite exhibited an extremely in a 6M KOH solution with an initial flow rate of 3 A/g, the Cs was 1256 F/g. Furthermore, high cyclic durability (after 3000 cycles 80% capacitance was retained), 62.8 Wh/kg optimum energy density, 7492.5 W/kg power density, specific capacity as well as decreased equivalent series resistance, were all shown by the three-dimensional electrode (0.58).

According to Zhou S et al., (2013), applying the zeolitic imidazolate framework-67 as a template, composite materials porosity Etching and coprecipitation are used to produce a hollow polyhedral nanocage made of $NiCo_2O_4$/$ZnCo_2O_4$/Co_3O_4. The presence of an artificial ligand in the templates may aid in the prevention of metal agglomeration This is due to the intense calcination, needed for the production of metallic nanostructure compounds with uniform particle sizes. The composite material's hollow nanocage structure uses a highly permeable infrastructure covering or framework, which provides a specific site & improves the redox reaction of the electrode's component. The nanocage has a Cs of 1892.5 F/g and 1135 F/g sequentially. The nanocage retains 66 % of its capacitance after successive 2000 cycles interpreted as good stability. Furthermore, the "$NiCo_2O_4$/ZCO/Co_3O_4/AC" hybrid system may be temporarily cycled across a possible range of 0.1-1.8 V and provide a greater voltage gain of 1.8 V and a maximum power density of 8006.67 W/kg. This research sheds light on the production of various composites and opens up new avenues for developing more attractive electrode materials.

3.1 Hydrothermal method

The hydrothermal method is a solution-based unique tool to prepare various nanostructures by simply varying temperature and time factors. In this technique, crystal growth is done between precursors within the steel autoclave. And required parameters are provided along with water. In hydrothermal technique morphology of prepared material can be varied by simply varying the pressure and concentration parameters of precursors. Some reputed groups reported ZCO combinations prepared via hydrothermal route are listed here. Reddy G et al., (2020) used a hydrothermal technique using polyvinylpyrrolidone to synthesize Peony-like 3D hierarchical ZCO formations with 2D nanoflakes. The reaction period was altered to get two samples, but the rest of the reaction conditions stayed the same. XRD analysis was used to study the crystalline characteristics of the structures, TEM and SEM were used to evaluate their morphologies, and X-ray photoelectron spectroscopy (XPS) was adapted to investigate the release of nutrients and oxidation states. The ZCO-6h sample has a compact pore size (24.69 nm) and a huge individual BET surface area (55.40 m^2/g), allowing for quicker charged particle transport than the ZCO-12h sample. The ZCO-12h electrode exhibited an excellent capacitive performance According to electrochemical tests, 421.05 F/g (31.52 C/g) has good cycle performance at 1 A/g. Furthermore, the morphologic properties of the hierarchy materials produced aided in the rise of Cs considerably. The outstanding capacitive results point to hierarchy 3D- ZCO peony-like structures constructed from two-dimensional materials as a potential material with high SCs.

A bunch of porous nanosheets with a thickness of 15 nm were built into ZCO hierarchical microspheres using a simple solvothermal method in a combined solvent comprising ethylene glycol (EG) and water, followed by a calcination procedure at 400 °C in air. The ZCO-modified electrode retained 98.7 % of the total of its initial Cs beyond 5000 stability cycles at 5 A/g, showing improved long-life endurance. The ZCO hierarchical microspheres' outstanding electrochemical properties make them a powerful and appropriate electro-active material for SC. The best ZCO HTNs, when used as the positive electrode in SCs, have an outstanding rate performance of 75.14%. Asymmetric SC made of ZCO HTNs and active carbon also exhibits steady or cycling behavior with ultra-high stability after completion of successive 20,000 stability cycles, with 95.38 % of its initial capacity. The present synthetic procedure is simple and does not need the use of costly chemicals or specialized equipment. By simply replacing the starting salts, the method may be used to synthesize. Nitrogen-doped activated carbon (PNAC) was effectively produced utilizing carbonized polyvinylidene fluoride as a carbon precursor through the hydrothermal nitrogen-doping technique, according to Wang W et. al., (2019). As a consequence, in a 2M KOH aqueous media, The PNAC electrodes have an outstanding range of performance and a large capacitor of 247 F/g at a current density of 0.5 A/g. Additionally, an all-solid-state asymmetrical SC (ASC) was also fabricated to utilize the gel electrolyte. In a sequence of two ASC, a red light may be produced. light-emitting diode, showing the SC's practical potential.

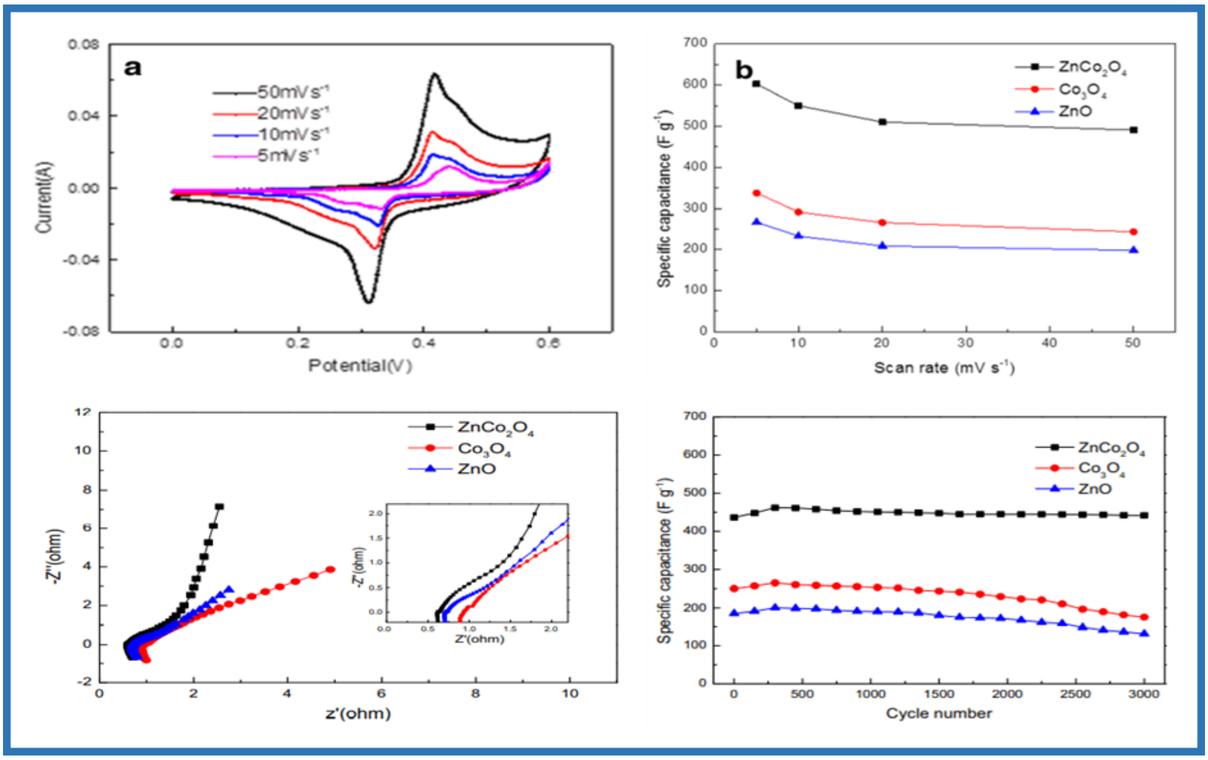

Fig. 8 a) a CV curves of ZCO at different scan rates **b)** Scan rate versus capacitance graph **c)** The EIS curves **d)** The electrochemical stability test of ZCO, Co_3O_4, and ZnO.

Saravanakumar B et al., (2015) stated that because of its larger surface area, excellent electrical conductivity, then enhanced electrode-electrolyte interface, the discovery of hierarchy, and porosity membrane-based current collectors have sparked a lot of attention in the areas of energy storage, sensing, then electrocatalysis. By using a dynamical hydrogen bubble template electro-deposition technique, we were able to create a hierarchical vascularised nanostructured porosity thin film as a current collector. For the first time, a porosity 3D-Ni adorned with Fe_2O_3 & ZCO has been reported using a simple, reduced electrochemical deposition technique. The porosity of 3D-Ni-based electrodes that were produced demonstrated outstanding electrochemical properties of high specific capacity, and good cycle stability. good cycle stability or good rate capability. The asymmetric solid-state SC device's negative or positive electrodes were constructed of porous, 3D Ni adorned with ZCO or Fe_2O_3. At a power density of (0.5 m/cm^2), the constructed Fe_2O_3 / $ZnCo_2O_4$ ASC device had aerial Cs of 92 mF/cm^2, a maximum power density of 3kW/cm^2, and 28.8 mWh/cm^2 of energy density. With the improved performance of porosity, 3D current collectors hold a lot of promise for the development of high-performance SCs.

Zhao et al., (2017) stated that in several large flexibility asymmetrical SC (ASC), lightweight, all-solid-state SCs, the positive electrode was cabbage-like ZCO, the negative electrode was porous VN nanowires, and the collector was elastic carbon nanotube film (CNTF). The positive electrode had the electrodes of the negative ion used to have a space capacitor of 400 mF/cm^2 and a major capacitor of 789.11 mF/cm^2. After manufacturing, some elastic ACs devices with resulting a Cs 196.43 mF/cm^{2,} as well as a voltage of 1.6 V seems to have outputs window flow rate, and 64.76 mWh/cm^3 energy density. Another output, or 64.76

mWh/cm^3 volumetric energy density, has a specific capacity of 196.43 mF/cm^2 successfully performs 2000 bending cycles, and the capacitance storage reached 95.7 %, demonstrating excellent flexibility and mechanical stability.

3.2 Reflux method

Reflux is a universal method for the synthesis of nanorods like template morphology, it is also a solution-based method to complete the transfer of ions through a solution on the substrate. It is the simplest and no vacuum required, easy instrumentation method. In reflux basically, heat is given to speed up the chemical reaction. The typical setup of reflux contains a round conical flask, a condenser, and heat provider assembly. The reflux technique is the cheapest method to synthesize nanostructure material. There are several groups that prepared ZCO by reflux tool. G.P. Kamble and the group (2021) prepared ZCO/NiO composite by reflux method delivered 85% Cs retention after 5000 cycles. Also, this composite exhibits a 134.79 m^2/g BET area, showing 882 F/g at a 4 mA/cm^2 current density. In asymmetric design with rGO, this design capable of delivering 46.66 Wh/kg energy per unit given mass and a power density is about 800 W/kg. A similar group also reported (2020) that ZCO nanorod prepared by a similar technique delivered 315 F/g at 2 mA/cm^2. Also, show an extraordinary energy density of 25.45 Wh/kg at 3620 W/kg power density in a 6M KOH electrolyte. This composite long lasting over 3000 cycles up to 77%. This was quite a good result in the electrochemistry field.

4. Performance of SC

According to Huang et al., (2015), the electrochemical performances of materials such as ZCO when utilized as SCs were thoroughly investigated using galvanostatic charge-discharge, EIS, and liner sweep cyclic voltammetry setup. ZCO's good cycling capabilities and large Cs suggest it is a good replacement for SCs. Using a topological transformation method, Bao J et al., (2018) presented an ultrathin configuration into spinel ZCO performances of the ZCO ultrathin nanosheets were also ascribed to the advantageous ultrathin structure, showing it as a viable option for energy storage and conversion applications.

In a commercial sponge, Moon IK et al., (2015) produced binary composites of ZCO and lowered graphene oxide (rGO). A hydrothermal method was used to generate ZCO nanosheets on the surface of the GO/sponge. In asymmetric SC. The $ZnCo_2O_4$/rGO/sponge electrodes, which exhibit outstanding electrochemical capabilities with a particular capacitance are used to build a flexible SC of all-solid-state compounds. The fabricated SC also has remarkable mechanical flexibility and cycling stability.

Sahoo S et al., (2017) used a hydrothermally assisted thermal annealing technique to produce Nanowire arrays as a cement SC electrode, ternary oxide/NiO (ZCGNO) on Ni foam ZCO/reduced graphene was used. Ni foam was used as the current collector, precursor, and NiO in that order. In a 6 M KOH solution, the resultant 3D ternary composite had an extreme Cs of 1256 F/g at a 3A/g current density. The electrochemical presentation of the three-dimensional electrode was likewise good. ZCGNO may be a viable alternative for excellent electrochemical characteristics.

Improvements in the inductance & energy level of materials based on zinc cobalt oxide, Sharma M et al., (2020), are critical for developing SCs with good electrochemical performance. To achieve outstanding supercapacitive performance, they used a simple hydrothermal technique to make Cu-doped zinc cobalt oxide nanostructures ($Zn_{1x}Cu_xCo_2O_4$) Lightweight and flexibility are two advantages, and they might be simply combined or weaved into a variety of electrical devices at a low cost and great efficiency. The electrochemical properties were studied using a two-electrode setup of the free-standing SC. Wu, Hao al., (2015), The SC has Cs was 10.9 F/g^1. The fiber SC also had a 76 mWh/kg energy density and

1.9 W/kg power density. metal adding Cu resulted in increased use a 2-fold higher surface area (52 m^2/g) and a charge transfer resistance is significantly decreased by 2-fold, which is 1.55 times more than the 917 F/g of the pure ZCO electrode. The $Zn_{0.7}Cu_{0.3}Co_2O_4$ maintains approximately 96% of its capacitance after a 1.5 V potential window and enhanced cycle stability. The finished device has a high specific capacity of 55C g^{-1} and 2621 W/kg power density and lights up yellow LED efficiently at 1.5 V. The significant effect in electrochemical performance may be ascribed to the increased electronic conductivity or surface area. The results revealed that the solid-state symmetric SC that was built was effective and may be utilized in future flexible energy storage systems.

Fibre electrochemical capacitors, according to Wu H et al., (2015), having lightweight and flexibility are two advantages, and they may be easily integrated or woven into a range of low-cost, high-efficiency electrical devices. This article offers a single-step hydrothermal method for manufacturing Simple and rapid conductivity is provided by nanorods of ZCO on a Ni wire. The ZCO hierarchical microspheres have outstanding electrochemical properties making them a promising and appropriate electro-active material for energy storage. The electrochemical assets of the unstructured SC were studied by applying a two-electrode configuration. The capacitance of a particular object of the SC was 10.9 F/g. The fiber SC also has a power density of 76 mWh/kg and a specific energy density tends to be 1.9 W/kg. When the flexible SC was bent at different angles, it showed exceptional electrochemical stability, indicating that it may be a better replacement as an electrode material for wearing energy storage applications**.**

Da He et al., (2020) suggested that the fine piqued attention for their possible use in SC applications. Bimetallic MOFs may offer a plethora of redox processes as a result of increased charge transfer among various metal ions, boosting enhance efficiency even further. Fig 2 shows how the “One-for-All” approach is used to make from such a single bimetallic MOF in this research. A simple technique was used to make the bimetallic Zn/Co-MOF with cuboid-like features. After post-heating the as-prepared Zn/Co-MOF and washing with HCl, nanoporous carbons (NPC) were produced, and bimetallic oxides (ZCO) were formed by sintering the Zn/Co-MOF in air. As negative and positive materials, MOF-derived NPC and bimetallic oxides were used to construct hybrid ASCs using 6 M KOH as an electrolyte.

5. Discussion

Because SCs are a necessary energy source, much research on the manufacture of functional SCs has been performed. Details of a few of the SCs made using ZCO alone or in conjunction with other metal, oxides are shown in Tables 2 & 3. Each produced SC's electrolytes, surface, voltage window, & effective conductance are listed in tables 2 & 3.

Table 2: A literature survey of $ZnCo_2O_4$-based supercapacitors in the two-electrode system measurement.

Positive electrode	Negative electrode	Electrolyte	Potential window	Specific capacitance	Energy density	Power density	Stability	Reference
ZCO/rGO/sponge	ZCO/ rGO/sponge	PVA - KOH	0 to 0.4 V	143 F/g at 1 A/g	11.44 Wh·/kg	0.143 kW·/kg	93.4% after 5000 cycles	Soundarya et al., 2021

Zn-Ni-Al-Co	AC	KOH	0–1.5 V	232 F/g at 0.5 A/g	72.4 Wh /kg	533 W /kg	90% after 10,000 cycles	Bhagwan et al., 2020
ZCO/C	AC	KOH	0 to 1.5 V	169 F/g at 1 A/g	45.9 Wh /kg	700 W /kg	95% after 9000 cycles	Liu et al., 2016
ZCO	ZCO	PVA /KOH	0-1.0 V	94 mF/ cm^2	–	–	100% after 1400 cycles	Fu et al., 2016
ZCO@ $Ni_xCo_{2x}(OH)_{6x}$	AC	KOH	0−1.7 V	-	26.2 Wh /kg	511.8 W /kg	88.2% after 2000 cycles	Attia et al., 2021
ZCO@ MnO_2	AC	KOH	0-1.6 V	197 F/g at 0.75 A/g	69 Wh /kg	4.9 kW /kg	93.5% after 5000 cycles	Heydari et al., 2017
ZCO	Fe_2O_3	KOH	0-1.6 V	92 mF/ cm^2 at 0.5 mA /cm^2	28.8 mW /cm^2	28.8 mWh /cm^2	-	Mohammed et al., 2017

ZCO	AC	KOH	0-1.4 V	-	28.2 Wh /kg	332.5 W /kg	91% after 3000 cycles	Zhou et al., 2018
ZCO	ZCO	PVA - KOH	0 - 1 V	69.65 F/g at 1.07 A/g[1]	9.67 Wh /kg	1.45 kW /kg	68 % after 2000 cycles	Wang et al., 2019
ZCO@NMiO4/Ni	CNTs/Ni	KOH	0 - 1.8 V	128 F/g at 1 A/g	57.5 Wh·/kg	18000 W/ kg	84.1 % after 10000 cycles	Wang et al., 2019
ZCO/PANI	ZCO/ PANI	KOH	0.0–1.0 V	103 F/g at 0.5 A/g	-	-	-	Saravanakumar et al., 2018
ZCO	AC	KOH	0-1.45 V	90 F/g at 1A/g	26.28 Wh /kg	716 W /kg	90 % after 5000 cycles	Zhao et al., 2017
Co_3O_4/ ZCO/CuO	AC	PVA - KOH	0-1.6 V	100.75 F/g at 1 A/g	35.82 Wh /kg	4799.25 W /kg	94% after 514 3000 cycles	Raut et al., 2017
ZCO	ZCO	PVA - KOH	0-0.5 V	2.243 mF $/cm^2$	areal 0.065 μWh $/cm^2$	0.092 mW $/cm^2$	99% after 2000 cycles	Wang et al., 2020

				at 0.025 mA /cm^2				
$NiCo_2O_4$/ ZCO/Co_3O_4	AC	PVA - KOH	0- 1.6 V	233.75 F/g at 1 A/g	83.11 Wh /kg	8006.67 W /kg	93.54 % after 3000 cycles	Shanmugavalli et al., 2019
ZCO	ZCO	KOH	0 to 1.5 V	5100 mF/ cm^2 at 0.2 A /m^2	31.8 mWh /cm^3	280 mW /cm^3	98% after 1000 cycles	Gungor et al., 2008
ZnO/ ZCO/NiO	AC	PVA - KOH	0– 1.6 V	129.5 F/g at 1 A/g	46.04 Wh /kg	7987.5 W /kg	104.17% after 5000 cycles.	Bhagwan et al., 2019
MWCNT @ZCO	AC	KOH	0- 1.45 V	17 mAh /g at 0.38 A /g	-	-	95% after 1000 cycles	Karthikeyan et al., 2009

ZCO/CNF	ZCO/CNF	KOH	0-1.2 V	77 F/g at 5 mV/s	-	1200 W /kg	98% after 100,000 cycles	Wu et al., 2015
ZCO	AC	KOH	0-1.5 V	182 F/g at 0.5 A/g	10.42 Wh /kg	375.12 W /kg	95.38% after 20 000 cycles	Yu et al., 2020
ZCO	ZCO	PVA /KOH	0-1 V	10.9 F/g at 10 mV /s	76 mWh /kg	1.9 W /kg	92% after 3500 cycles	Omar et al., 2017
ZCO@ $CoMoO_4$	AC	KOH	0-1.6 V	82.24 F/g at 5 mA /cm^2	29.24 W h /kg	10526.32 W /kg	90.95% after 5000 cycles	Gai et al., 2017
PANI-ZCO	AC	KOH	0-1.5 V	64 C/g at 0.5 A/g	13.25 Wh /kg	375 W /kg	90% after 3000 cycles	Javed et al., 2019
ZCO	AC	PVA /KOH	0-1.4 V	80.71 F/g at 0.2 A/g	21.97 W /kg	972.22 W /kg	76.68% after 1000 cycles	Bhagwan et al., 2020

ZCO@ NiMoO4	AC	KOH	0 - 1.6 V	71.3 F/g at 5 mA /cm^2	25.3 W h /kg	9467.5 W /kg	85.1% after 5000 cycles	Meng, et al., 2020
ZCO@Co –Al LDH	AC	PVA – KOH	0- 1.6 V	139.2 F/g at 0.5 A/g	50.1 Wh /kg	6200 W /kg	90.5% after 3200 cycles	Bai, et al., 2019
$ZnCo_2S_4$/ ZCO	CNTs	KOH	0- 1.5 V	130 F/g at 1 A/g	127.4 Wh /kg	2520 W /kg	89% after 5000 cycles	Wang et al., 2020
ZCO@N CS-6	AC	KOH	0- 1.7 V	92.4 F/g at 0.5 A/g	37.1 W h /kg	5124.3 W /kg	90.29% after 8000 cycles	Xuan et al., 2020
ZCO/$Ni_3V_2O_8$	AC	KOH	0- 1.6 V	253 F/g at 1 A/g	90 Wh /kg	812 W /kg	82% after 5000 cycles	Huang et al., 2019
ZCO@$ZnWO_4$	AC	KOH	0- 1.6 V	-	24 Wh /kg	2001.07 W /kg	98.5% after 5000 cycles	Xie et al., 2018
$Zn_{0.7}Cu_{0.3}Co_2O_4$	$Zn_{0.7}Cu_{0.3}Co_2O_4$	PVA – KOH	0- 1.5 V	175 F/g at 3.5 A/g	55 W h /kg	2621 W /kg	72% after 5000 cycles	Sharma et al., 2020

ZCO	ZCO	KOH	0−1 V	340 F/g at 1 A /g	11.8 Wh /kg	2.5 kW /kg	-	Rajesh et al., 2016

Table 3: A literature survey of $ZnCo_2O_4$-based supercapacitors in the three-electrode system measurement.

Electrode	Electrolyte	Potential window	Surface area	Specific capacitance/capacity	Stability	Reference
ZCO/rGO/sponge	KOH	-0.2 to +0.3 V	_	1116.6 F/g	_	Soundarya et al., 2021
Zn-Ni-Al-Co	KOH	0.1 and 0.5 V	83.5 m^2 /g	839.2 C/g at 1 A/g	82% after 5000 cycles	Bhagwan et al., 2020
ZCO/C	KOH	0-0.6 V	-	1821 F/g at 5 A/g	100 % after 9000 cycles	Liu et al., 2016
ZCO	KOH	0-0.4 V	-	1400 F/g at 1 A/g	97 % after 1000 cycles	Fu et al., 2016

ZCO@ $Ni_xCo_{2x}(OH)_{6x}$	KOH	-0.1–0.5 V	-	419.1 µAh /cm^2 at 5 mA/cm^2	81.4% after 2000 cycles	Attia et al., 2021
ZCO-MnO_2	KOH	-0.1 to 0.5 V	-	2057 F/g at 1 A/g	96.5% after 5000 cycles	Heydari et al., 2017
ZCO	KOH	0 to 0.6 V	138.8 m^2 /g	1781.7 F/g at 5 A/g	92 % after 4000 cycles	Heydari et al., 2016
ZCO	KOH	0–0.7 V	-	1170 F/g at 2 A/g	95% after 3000 cycles	Saravanakumar et al., 2018
ZCO	KOH	0-0.4 V	23.13 m^2 /g	1596 F/g at 1 A/g	119% after 2000 cycles	Mohamed et al., 2017
ZCO	KOH	0 - 0.5 V	-	675 F/g at 3.5 A/g	71% after 2000 cycles	Raut et al., 2016
ZCO@$NMioO_4$	KOH	0 - 0.5 V	-	1912 F/g at 1 A/g	55% at 20 A/g	Wang et al., 2019

ZCO	KOH	0 - 0.45 V		711 F/g at 0.5 A/g	92.5% after 1000 cycles	Shanmugavalli et al., 2019
ZCO/PANI	KOH	0 - 0.45 V		867 F/g at 0.5 A/g	98.9% after 1000 cycles	Saravanakumar et al., 2018
ZCO	KOH	0 - 0.45 V	77 m^2 /g	843 F/g at 1 A/g	97 % after 5000 cycles	Zhao et al., 2017
Co_3O_4/ ZCO/CuO	KOH	0-0.6 V	73.6 m^2 /g	890.2F/g at 1 A/g	89.7% after 1000 cycle	Raut et al., 2017
ZCO	KOH	0-0.6 V	-	604.52 F/g at 1 A/g	95.62 % after 3000 cycles	Wang et al., 2020
ZCO/Ni foam coated with graphene	KOH	0 - 1V	184 m^2 /g	1626 F/g at 1 A/g	88.7% after 5000 cycles	Lv et al., 2017

ZCO	KOH	0-0.4V	-	305 F/g at 2A/g	92% after 10,000 cycles	Huang et al., 2018
$NiCo_2O_4$/ZCO/Co_3O_4	KOH	0 - 0.5 V	73.89 m^2 /g	1892.5 F/g at 1 A/g	66% after 2000 cycles	Shanmugavalli et al., 2019
ZCO	KOH	0.05-0.45V	55 m^2 /g	451 F/g at 0.2 A/m^2	97.9% after 1500 cycles	Gungor et al., 2008
ZnO/ZCO/NiO	KOH	0 to 0.7 V	29.9 m^2 /g	1136.4 F/g at 1 A/g	86.54% after 5000 cycles	Bhagwan et al., 2019
ZCO	KOH	0.0 - 0.45 V	-	37 mAh/g at 1 A/g	-	Bhagwan et al., 2019
MWCNT@ZCO	KOH	0.0 - 0.45 V	-	64 mAh/g at 1 A/g	88% after 2000 cycles	Karthikeyan et al., 2008
ZCO/C	KOH	0- 0.6 V	199.0 m^2 /g	327.5 F/g at 0.5 A/g	125% after 1000 cycles	Yu et al., 2020

ZCO@$NiCo_2O_4$	KOH	0- 0.7 V	-	1476 F/g at A/g	98.9% after 2000 cycles	Huang et al., 2015
ZCO	KOH	0 - 0.6V	-	770 F/g at 10 A/g	89.5% after 3000 cycles	Zhou et al., 2014
ZCO	KOH	0-0.5V	34.191 m^2 /g	181 C/g at 0.5 A/g	97.42% after 10 000 cycles	Zhao et al., 2020
CC@ZCO@MnO_2	KOH	0-0.7V	-	3.6 F/cm^2 at 2 mA/cm^2	95.5% after 5000 cycles	Lin et al., 2016
ZCO@$CoMoO_4$	KOH	0 to 0.6 V	-	1096.08 C /g at 10 mA /cm^2	104.1% after 5000 cycles	Meng et al., 2020
PANI-ZCO	KOH	0-0.5V	-	398 C/g at 1 A/g	-	Javed et al., 2019
ZCO	KOH	0-0.7V	34.60 m^2 /g	542.5 F/g at 1 A/g	95.5% after	Bhagwan et al., 2020

					2000 cycles	
ZCO@$NiMoO_4$	KOH	0-0.6V	-	1238.1 C/g at 3 mA /cm^2	103.4% after 5000 cycles	Meng et al., 2019
ZCO@Co–Al LDH	KOH	0 - 0.7 V	-	2041 F/g at 1 A/g	-	Bai et al., 2019
$ZnCo_2S_4$/ZCO	KOH	0-0.5V	-	1057.78 F/g at 1 A/g	-	Wang et al., 2019
ZCO@NCS-6	KOH	0-0.7V	-	1762.6 F/g at 1A/g	81.4% after 5000 cycles.	Xuan et al., 2020
ZCO/$Ni_3V_2O_8$	KOH	0-0.6V	-	1734 F/g at 1A/g	96% after 8000 cycles	Huang et al., 2019
S-ZCO	KOH	0–0.5 V	-	214.1C/g at 0.5 A/g	78% after 5000 cycles	Yang et al., 2020
ZCO	KOH	0-0.9V	63.4 m^2 /g	2468 F/g at 5 A/g	96.3% after	Bao et al., 2013

					1500 cycles	
$ZCO@ZnWO_4$	KOH	0–0.5 V	-	13.4 F/cm^2 at 4 mA /cm^2	-	Xie et al., 2013
$Zn_{0.7}Cu_{0.3}Co_2O_4$	KOH	0−5 V	52 m^2 /g	1425 F/g at A/g	96% after 2000 cycles	Sharma et al., 2020
ZCO	KOH	0−0.5 V	37.27 m^2 /g	853.6 F/g at 2 A/g	92.7% after 3000 cycles	Rajesh et al., 2016

6. Conclusion

supercapacitors, also called electrolytic devices, must have been contemplated as a possible electrochemical energy storage technology because tofts aid in long-life cycle durability, supercharging operation, environmentally friendly nature, and high-power density. Consequently, in recent years, engineers and scientists have started paying careful attention to ZCO-based supercapacitors. Various synthetic techniques have been used to create microspheres, nanorods, nanoparticles (NPs), nanoflakes, hexagonal-like structures, nanowires (NWs), and other ZCO micro/nanostructures, which have previously been used as electrode materials. Various manufacturing techniques & combinations of other compounds with ZCO have been discovered to improve the performance of the device. However, other techniques must be explored further in terms of improving the electrochemical behavior of ZCO materials. This review gives a basic track to new researchers about choosing ZCO as an efficient electrode material for supercapacitors.

Declaration of Competing Interest:

The authors declare that they have no known competing financial interests or personal relationships that could have appeared to influence the work reported in this paper.

Acknowledgment:

The authors are grateful to the Mahatma Jyotiba Phule Research Fellowship (MJPRF 2021) for funding. Authors would also like to acknowledge Rayat Institute of Research and Development (RIRD) Satara, Maharashtra, India for providing kind support during this study.

References

Attia, S. Y., Mohamed, S. G., Barakat, Y. F., Hassan, H. H., & Al Zoubi, W. (2021). Supercapacitor electrode materials: Addressing challenges in mechanism and charge storage. Reviews in Inorganic Chemistry.

Bao, F., Wang, X., Zhao, X., Wang, Y., Ji, Y., Zhang, H., & Liu, X. (2014). Controlled growth of mesoporous $ZnCo_2O_4$ nanosheet arrays on Ni foam as high-rate electrodes for supercapacitors.

Bao, J., Wang, Z., Liu, W., Xu, L., Lei, F., Xie, J., ... & Li, H. (2018). $ZnCo_2O_4$ ultrathin nanosheets towards the high performance of flexible supercapacitors and bifunctional electrocatalysis. Journal of Alloys and Compounds, 764, 565-573.

Bhagwan, J., Hussain, S. K., & Yu, J. S. (2020). Aqueous asymmetric supercapacitors based on ZnCo2O4 nanoparticles via facile combustion method. Journal of Alloys and Compounds, 815, 152456.

Bhagwan, J., Nagaraju, G., Ramulu, B., & Yu, J. S. (2019). Promotive effect of MWCNT on ZnCo2O4 hexagonal plates and their application in aqueous asymmetric supercapacitor. Journal of The Electrochemical Society, 166(2), A217.

Chen, L., Jiao, Y., Li, Z., & Gao, Y. (2019). Controllable fabrication of $ZnCo_2O_4$ ultra-thin curved sheets on Ni foam for high-performance asymmetric supercapacitors. Electrochimica Acta, 299, 388-394.

Chen, S., Zhu, J., Han, Q., Zheng, Z., Yang, Y., & Wang, X. (2009). Shape-controlled synthesis of one-dimensional MnO2 via a facile quick-precipitation procedure and its electrochemical properties. Crystal Growth & Design, 9(10), 4356-4361.

Cheng, H., Lu, Z. G., Deng, J. Q., Chung, C. Y., Zhang, K., & Li, Y. Y. (2010). A facile method to improve the high rate capability of Co3O4 nanowire array electrodes. Nano Research, 3(12), 895-901.

Cheng, J., Lu, Y., Qiu, K., Yan, H., Hou, X., Xu, J., ... & Luo, Y. (2015). Mesoporous $ZnCo_2O_4$ nanoflakes grown on nickel foam as electrodes for high-performance supercapacitors. Physical Chemistry Chemical Physics, 17(26), 17016-17022.

Conway, B. E. (2013). Electrochemical supercapacitors: scientific fundamentals and technological applications. Springer Science & Business Media.

Dubal, D. P., Gund, G. S., Holze, R., Jadhav, H. S., Lokhande, C. D., & Park, C. J. (2013). The solution-based binder-free synthetic approach of RuO2 thin films for all-solid-state supercapacitors. Electrochimica Acta, 103, 103-109.

Frackowiak, E., Metenier, K., Bertagna, V., & Beguin, F. (2000). Supercapacitor electrodes from multiwalled carbon nanotubes. Applied Physics Letters, 77(15), 2421-2423.

Fu, W., Wang, Y., Han, W., Zhang, Z., Zha, H., & Xie, E. (2016). Construction of hierarchical $ZnCo_2O_4$@ $Ni_xCo_{2x}(OH)_{6x}$ core/shell nanowire arrays for high-performance supercapacitors. Journal of Materials Chemistry A, 4(1), 173-182.

Gai, Y., Shang, Y., Gong, L., Su, L., Hao, L., Dong, F., & Li, J. (2017). A self-template synthesis of porous $ZnCo_2O_4$ microspheres for high-performance quasi-solid-state asymmetric supercapacitors. RSC advances, 7(2), 1038-1044.

Güngör, K., & Karthikeyan, K. G. (2008). Phosphorus forms and extractability in dairy manure: a case study for Wisconsin on-farm anaerobic digesters. Bioresource Technology, 99(2), 425-436.

Guo, D., Zhang, H., Yu, X., Zhang, M., Zhang, P., Li, Q., & Wang, T. (2013). Facile synthesis and excellent electrochemical properties of $CoMoO_4$ nanoplate arrays as supercapacitors. Journal of Materials Chemistry A, 1(24), 7247-7254.

He, Y. B., Li, G. R., Wang, Z. L., Su, C. Y., & Tong, Y. X. (2011). Single-crystal ZnO nanorod/amorphous and nanoporous metal oxide shell composites: Controllable electrochemical synthesis and enhanced supercapacitor performances. Energy & Environmental Science, 4(4), 1288-1292.

Heydari, H., & Gholivand, M. B. (2017). Novel synthesis and characterization of ZnCo2O4 nanoflakes grown on nickel foam as efficient electrode materials for electrochemical supercapacitors. Ionics, 23(6), 1489-1498.

Hou, L., Hua, H., Liu, S., Pang, G., & Yuan, C. (2015). Surfactant-assisted hydrothermal synthesis of ultrafine $CoMoO_4 \cdot_{0.9} H_2O$ nanorods towards high-performance supercapacitors. New Journal of Chemistry, 39(7), 5507-5512.

Huang, C., Hao, C., Ye, Z., Zhou, S., Wang, X., Zhu, L., & Wu, J. (2019). In situ growth of ZIF-8-derived ternary $ZnO/ZnCo_2O_4/NiO$ for high-performance asymmetric supercapacitors. Nanoscale, 11(20), 10114-10128.

Huang, Y., Miao, Y. E., Lu, H., & Liu, T. (2015). Hierarchical $ZnCo_2O_4$@ $NiCo_2O_4$ Core–Sheath Nanowires: Bifunctionality towards High-Performance Supercapacitors and the Oxygen-Reduction Reaction. Chemistry-A European Journal, 21(28), 10100-10108.

Javed, M. S., Lei, H., Shah, H. U., Asim, S., Raza, R., & Mai, W. (2019). Achieving high rate and high energy density in an all-solid-state flexible asymmetric pseudocapacitor through the synergistic design of binder-free 3D $ZnCo_2O_4$ nano polyhedra and 2D layered Ti 3 C 2 T x-MXenes. Journal of Materials Chemistry A, 7(42), 24543-24556.

Kaliaraj, G. S., & Ramadoss, A. (2020). Nickel–zinc sulfide nanocomposite thin film as an efficient cathode material for high-performance hybrid supercapacitors. Materials Science in Semiconductor Processing, 105, 104709.

Kamble, G. P., Kashale, A. A., Kolekar, S. S., Chen, I. W., Sathe, B. R., & Ghule, A. V. (2021). Reflux temperature-dependent zinc cobaltite nanostructures for asymmetric supercapacitors. *Journal of Materials Science: Materials in Electronics*, *32*(5), 5859-5869.

Kamble, G. P., Rasal, A. S., Chang, J. Y., Kolekar, S. S., Tayade, S. N., & Ghule, A. V. (2022). Structure-engineering of core–shell ZnCo 2 O 4@ NiO composites for high-performance asymmetric supercapacitors. *Nanoscale Advances*.

Karthikeyan, K., Kalpana, D., & Renganathan, N. G. (2009). Synthesis and characterization of ZnCo2O4 nanomaterial for symmetric supercapacitor applications. Ionics, 15(1), 107-110.

Kumbhar, V. S., & Kim, D. H. (2018). Hierarchical coating of MnO2 nanosheets on ZnCo2O4 nanoflakes for the enhanced electrochemical performance of asymmetric supercapacitors. Electrochimica Acta, 271, 284-296.

Leitner, K., Lerf, A., Winter, M., Besenhard, J. O., Villar-Rodil, S., Suarez-Garcia, F., ... & Tascon, J. M. D. (2006). Nomex-derived activated carbon fibers as electrode materials in carbon-based supercapacitors. Journal of power sources, 153(2), 419-423.

Li, X., Shao, J., Li, J., Zhang, L., Qu, Q., & Zheng, H. (2013). Ordered mesoporous MoO2 as a high-performance anode material for aqueous supercapacitors. Journal of power sources, 237, 80-83.

Li, X., Xiong, S., Li, J., Bai, J., & Qian, Y. (2012). Mesoporous NiO ultrathin nanowire networks too tactically transformed from α-Ni (OH) 2 hierarchical microspheres and their superior electrochemical capacitance properties and excellent capability for water treatment. Journal of Materials Chemistry, 22(28), 14276-14283.

Liu, B., Liu, B., Wang, Q., Wang, X., Xiang, Q., Chen, D., & Shen, G. (2013). New energy storage option: toward ZnCo2O4 nanorods/nickel foam architectures for high-performance supercapacitors. ACS applied materials & interfaces, 5(20), 10011-10017.

Lu, X., Zheng, D., Zhai, T., Liu, Z., Huang, Y., Xie, S., & Tong, Y. (2011). Facile synthesis of large-area manganese oxide nanorod arrays as a high-performance electrochemical supercapacitor. Energy & Environmental Science, 4(8), 2915-2921.

Mary, A. J. C., Sathish, C. I., Kumar, P. S. M., Vinu, A., & Bose, A. C. (2020). Fabrication of hybrid supercapacitor device based on NiCo2O4@ ZnCo2O4 and the biomass-derived N-doped activated carbon with a honeycomb structure. Electrochimica Acta, 342, 136062.

Mohamed, S. G., Attia, S. Y., & Allam, N. K. (2017). One-step, calcination-free synthesis of zinc cobaltite nanospheres for high-performance supercapacitors. Materials today energy, 4, 97-104.

Moon, I. K., Yoon, S., Chun, K. Y., & Oh, J. (2015). Highly elastic and conductive n-doped monolithic graphene aerogels for multifunctional applications. Advanced Functional Materials, 25(45), 6976-6984.

Omar, F. S., Numan, A., Duraisamy, N., Bashir, S., Ramesh, K., & Ramesh, S. (2017). A promising binary nanocomposite of zinc cobaltite intercalated with polyaniline for supercapacitor and hydrazine sensor. Journal of Alloys and Compounds, 716, 96-105.

Pan, Y., Gao, H., Zhang, M., Li, L., & Wang, Z. (2017). Facile synthesis of $ZnCo_2O_4$ micro-flowers and micro-sheets on Ni foam for pseudocapacitor electrodes. Journal of Alloys and Compounds, 702, 381-387.

Pandolfo, A. G., & Hollenkamp, A. F. (2006). Carbon properties and their role in supercapacitors. Journal of power sources, 157(1), 11-27.

Raut, S. S., & Sankapal, B. R. (2017). Porous zinc cobaltite (ZnCo2O4) film by successive ionic layer adsorption and reaction towards solid-state symmetric supercapacitor device. Journal of Colloid and Interface Science, 487, 201-208.

Sahoo, S., & Shim, J. J. (2017). Facile synthesis of three-dimensional ternary ZnCo2O4/reduced graphene oxide/NiO composite film on nickel foam for next-generation supercapacitor electrodes. ACS Sustainable Chemistry & Engineering, 5(1), 241-251.

Saravanakumar, B., Ko, T. H., & Kim, B. S. (2018). Rational design of binder-free ZnCo2O4 and Fe2O3 decorated porous 3D Ni as high-performance electrodes for asymmetric supercapacitor. Ceramics International, 44(9), 10635-10645.

Shanmugavalli, V., & Vishista, K. (2019). Low-cost synthesis of cubic spinel structured high efficient NiCo2O4/polyaniline nanocomposite for supercapacitor application. Materials Research Express, 6(4), 045021.

Shao, M., Ning, F., Zhao, Y., Zhao, J., Wei, M., Evans, D. G., & Duan, X. (2012). Core-shell layered double hydroxide microspheres with tunable interior architecture for supercapacitors. Chemistry of Materials, 24(6), 1192-1197.

Sharma, M., Gaur, A., & Quamara, J. K. (2020). Swift heavy ions irradiated PVDF/BaTiO3 film as a separator for supercapacitors. Solid State Ionics, 352, 115342.

Sharma, Y., Sharma, N., Rao, G. S., & Chowdari, B. V. R. (2009). Nano-(Cd 1/3 Co 1/3 Zn 1/3) CO 3: a new and high-capacity anode material for Li-ion batteries. Journal of Materials Chemistry, 19(28), 5047-5054.

Simon, P., & Gogotsi, Y. (2010). Materials for electrochemical capacitors. In Nanoscience and technology: a collection of reviews from Nature journals (pp. 320-329).

Soundarya, G. G., Nalini, B., Lakshmi, D., & Priyanka, P. (2021). Structural rearrangement by Ni, Cr doping in zinc cobaltite and its influence on super capacitance. Ceramics International, 47(13), 18635-18645.

Sugimoto, W., Iwata, H., Yokoshima, K., Murakami, Y., & Takasu, Y. (2005). Proton and electron conductivity in hydrous ruthenium oxides evaluated by electrochemical impedance spectroscopy: the origin of large capacitance. The Journal of Physical Chemistry B, 109(15), 7330-7338.

Wang, J. G., Jin, D., Zhou, R., Li, X., Liu, X. R., Shen, C., ... & Wei, B. (2016). Highly flexible graphene/Mn3O4 nanocomposite membrane as advanced anodes for Li-ion batteries. ACS Nano, 10(6), 6227-6234.

Wang, J., Wang, S., Tian, Y., Jin, X., & Dong, J. (2020). 3D heterogeneous $ZnCo_2O_4$@ $NiMoO_4$ nanoarrays grown on Ni foam as a binder-free electrode for high-performance energy storage. Journal of Energy Storage, 32, 101899.

Wang, W., Zhang, N., Ye, Z., Hong, Z., & Zhi, M. (2019). Synthesis of 3D hierarchical porous Ni-Co layered double hydroxide/N-doped reduced graphene oxide composites for supercapacitor electrodes. Inorganic Chemistry Frontiers, 6(2), 407-416.

Wei, L., Sevilla, M., Fuertes, A. B., Mokaya, R., & Yushin, G. (2012). Polypyrrole-derived activated carbons for high-performance electrical double-layer capacitors with ionic liquid electrolyte. Advanced Functional Materials, 22(4), 827-834.

Winter, M., & Brodd, R. J. (2004). What are batteries, fuel cells, and supercapacitors? Chemical Reviews, 104(10), 4245-4270.

Wu, H., Jiang, K., Gu, S., Yang, H., Lou, Z., Chen, D., & Shen, G. (2015). Two-dimensional Ni (OH) 2 nanoplates for flexible on-chip micro-supercapacitors. Nano Research, 8(11), 3544-3552.

Wu, H., Lou, Z., Yang, H., & Shen, G. (2015). A flexible spiral-type supercapacitor based on ZnCo 2 O 4 nanorod electrodes. Nanoscale, 7(5), 1921-1926.

Wu, X., Meng, L., Wang, Q., Zhang, W., & Wang, Y. (2019). Highly flexible and large areal/volumetric capacitances for asymmetric supercapacitor based on $ZnCo_2O_4$ nanorods arrays and polypyrrole on carbon cloth as binder-free electrodes. Materials Letters, 234, 1-4.

Xing, W., Li, F., Yan, Z. F., & Lu, G. Q. (2004). Synthesis and electrochemical properties of mesoporous nickel oxide. Journal of power sources, 134(2), 324-330.

Xu, K., Chao, J., Li, W., Liu, Q., Wang, Z., Liu, X., ... & Hu, J. (2014). $CoMoO_4$· 0.9 H 2 O nanorods grown on reduced graphene oxide as advanced electrochemical pseudocapacitor materials. RSC Advances, 4(65), 34307-34314.

Yu, D., Teng, Y., Liu, X., & Liu, X. (2020). A high-performance electrode based on the ZnCo2O4@ CoMoO4 core-shell nanosheet arrays on nickel foam and their application in a battery-supercapacitor hybrid device. Electrochimica Acta, 347, 136278.

Zhang, X., Wang, J., Liu, J., Wu, J., Chen, H., & Bi, H. (2017). Design and preparation of a ternary composite of graphene oxide/carbon dots/polypyrrole for supercapacitor application: Importance and unique role of carbon dots. Carbon, 115, 134-146.

Zhao, H., Liu, L., Vellacheri, R., & Lei, Y. (2017). Recent advances in designing and fabricating self-supported nanoelectrodes for supercapacitors. Advanced Science, 4(10), 1700188.

Zhao, S., Yu, X., Chen, H., Tao, K., Hu, Y., & Han, L. (2020). Zeolitic imidazolate framework derived $ZnCo_2O_4$ hollow tubular nanofibers for long-life supercapacitors. RSC advances, 10(23), 13922-13928.

Zhou, S., Ye, Z., Hu, S., Hao, C., Wang, X., Huang, C., & Wu, F. (2018). Designed formation of $Co_3O_4/ZnCo_2O_4/CuO$ hollow polyhedral nanocages derived from zeolitic imidazolate framework-67 for high-performance supercapacitors. Nanoscale, 10(33), 15771-15781.

Zou, R., Xu, K., Wang, T., He, G., Liu, Q., Liu, X., ... & Hu, J. (2013). Chain-like NiCo 2 O 4 nanowires with different exposed reactive planes for high-performance supercapacitors. *Journal of Materials Chemistry A*, *1*(30), 8560-8566.